Available online at www.sciencedirect.com
ScienceDirect
Applied Surface Science 253 (2007) 3664–3668
applied surface science
www.elsevier.com/locate/apsusc

Helical nanostructures of SiO_x synthesized through the heating of Co-coated substrates

Hyoun Woo Kim *, Seung Hyun Shim

School of Materials Science and Engineering, Inha University, Incheon 402-751, Republic of Korea

Received 1 July 2006; received in revised form 27 July 2006; accepted 27 July 2006
Available online 12 September 2006

Abstract

This paper presents the use of the simple annealing technique at 1000 °C to produce the helical nanostructures of SiO_x. We have employed the Co-coated Si substrates, with Co layer and Si substrate utilized as catalyst and Si source, respectively. Beside the ordinary straight nanowires, the helical nanowires such as nanosprings and nanorings were observed. The product was an amorphous structure of SiO_x. We have discussed the possible growth mechanism. Photoluminescence spectrum of the SiO_x nanostructures showed a blue emission at 428 nm and a green emission at 534 nm, respectively.

PACS: 61.46.+w; 78.55.−m; 81.07.−b

Keywords: Nanostructures; Chemical synthesis; Transmission electron microscopy

1. Introduction

Since one-dimensional (1D) structures in the form of tubes, wires, and belts have attracted much attention because of their interesting geometries, novel properties, and potential applications [1–4], considerable efforts have been placed on the synthesis and characterization of those materials over the past several years. It has been shown that nano- and micron-scale 1D structures grow in a variety of configurations ranging from straight to helical. The helical structures, owing to their interesting morphology, as well as mechanical [5], electrical [6], and electromagnetic properties, potential applications of these nanostructures include micro and nanoelectromechanical systems (MEMS and NEMS) such as springs, magnetic field detectors, chemical or biological sensors, electromagnets, inductors, actuators, and high-performance electromagnetic wave absorbers. Accordingly, many helical structures have been synthesized from different materials, including carbon micro-coils based on amorphous carbon [7], carbon nanocoils based on carbon nanotubes [8], ZnO helical structures consisting of nanobelts [9,10], SiO_x-based nanosprings [11,12], SiC nanosprings [13], Si_3N_4 spring-like fibers [14], and amorphous BC nanosprings [15]. Si and SiO_x nanostructures have attracted considerable attention due to their unique properties and promising application in mesoscopic research, nanodevices, and opto-electronics devices [16–18]. Particularly, SiO_x is an important material for photoluminescence (PL) [19,20]. Therefore, the synthesis of SiO_x helical nanostructures is important not only for scientific interests but also for future industrial applications.

Since the majority of SiO_x nanowires fabrication methods are catalyst-based methods, metal catalysts such as Au [11] and Fe [12] have been used for the production of SiO_x helical nanostructures. Although Co has been one of the most utilized catalyst for the growth of carbon nanotubes [21], to our best knowledge, synthesis of inorganic nanostructure on Co substrates has been rarely reported to date. In this paper, we report the production of SiO_x nanowires by the simple heating of Co-coated Si substrates. The present synthetic route did not use an additional Si source other than Si substrate, different from the previous experiments for the growth of SiO_x helical nanostructures [11,12] and the development of simple growth technique will contribute to the potential applications of SiO_x helical nanostructures. We discuss the possible growth mechanism with respect to the role of the predeposited Co layers.

* Corresponding author. Tel.: +82 32 860 7544; fax: +82 32 862 5546.
E-mail address: hwkim@inha.ac.kr (H.W. Kim).

0169-4332/$ – see front matter © 2006 Elsevier B.V. All rights reserved.
doi:10.1016/j.apsusc.2006.07.083

2. Experimental

The growth process was carried out in a quartz tube. The experimental apparatus has been described elsewhere [22]. We have employed Co-coated Si substrates. In order to fabricate the Co-coated Si substrates, we used Si as starting materials onto which a layer of Co (approximate thickness = 5 nm) was deposited by the sputtering.

On top of the alumina boat, a piece of the substrate was placed with the Co-coated side downwards. The quartz tube was inserted into a horizontal tube furnace. During the experiment, a constant pressure with an air flow (~2.1% O_2 in a balance of argon) was maintained at 200 mTorr. The substrate temperature was set to 1000 °C. After 2 h of typical heating process, the substrate was cooled down and then removed from the furnace for analysis.

The crystal structure of the product was examined by means of glancing angle (0.5°) X-ray diffraction (XRD; X'pert MPD-Philips). The morphologies of the samples were checked by scanning electron microscopy (SEM, Hitachi S-4200) and transmission electron microscopy (TEM, Philips CM-200). Energy-dispersive X-ray analysis (EDX), which was attached to TEM, was employed for identifying the elemental compositions of the product. TEM samples were prepared by the following procedure: A small piece of film was stripped off and dispersed in acetone with the aid of ultrasonic vibration for about 5 min, and then a drop of solution was added to a copper microgrid covered by holey carbon.

3. Results and discussion

Fig. 1a shows the SEM top view of the sample morphology on the Co-coated Si substrates. The dominant component of the as-synthesized product is nanowires with a straight and smoothly curved parts, but a significant amount of nanowires has ring shape (arrow 1 in a) or spring shape (arrow 2 in a). Although the nanowires have a high ratio of length to diameter, the diameter remains nearly the same throughout the nanowire. Statistical observation of many SEM images indicated that the average diameter of nanowires varied from 20 to 100 nm. A well-formed nanospring is shown in Fig. 1b. In this spring-like nanostructure, the nanowire coiled regularly with an average coil pitch of 50–100 nm, a coil diameter of 120–220 nm, and a coil length of approximately 2 μm. The average diameter of the nanowires in this particular nanospring ranges from 40 to 70 nm. Fig. 1c shows another nanospring with a coil diameter of 170–250 nm. The average diameter of the nanowires ranges from 45 to 90 nm. It is noteworthy that the coil pitch is almost the same with the nanowire diameter. SEM images reveal that the nanosprings grown in the present study consist of single nanowires, rather than multiple nanowires. Fig. 1d shows the representative SEM image of ring-shaped helical nanostructures (indicated by arrow 3). Fig. 1e shows the XRD patterns of the product, revealing that the nanowires are fully amorphous. In the XRD measurements, the angle of the incident beam to the substrate surface was approximately

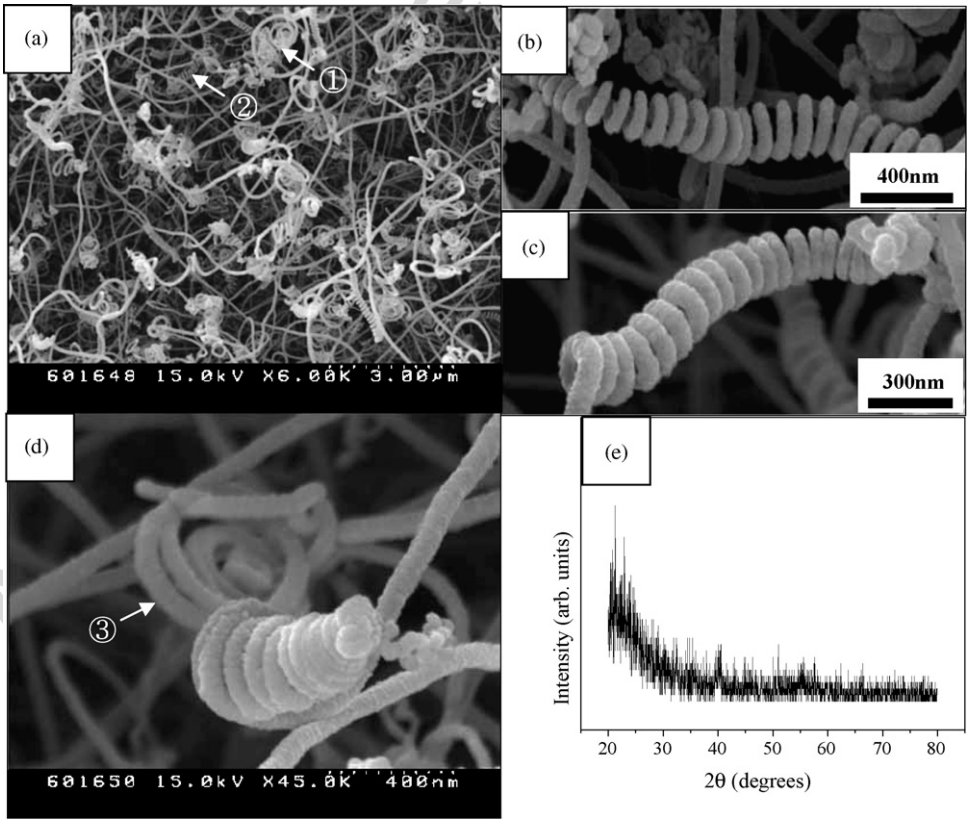

Fig. 1. (a) SEM image representing the morphology of product. Arrows 1 and 2 indicate the nanorings and the nanosprings, respectively. Enlarged views of (b and c) nanosprings and (d) nanorings (arrow 3). (e) XRD pattern of the product.

0.5°, and the detector was rotated to scan the samples. Therefore, we surmise that the spectrum is mainly from the product.

TEM was employed to further analyze the morphology of individual nanostructures. Fig. 2a shows the low-magnification TEM image, revealing the existence of various nanostructures including nanosprings, nanorings, as well as nanowires with straight or smoothly curved morphology. As shown in the inset of Fig. 2a, the highly dispersed selected area electron diffraction (SAED) pattern indicates that the nanostructures are amorphous. Fig. 2b shows a TEM image representing a nanospring consisting of a single nanowire with a diameter in the range of 25–35 nm, where the coil diameter and its pitch are 120–200 and 50–140 nm, respectively.

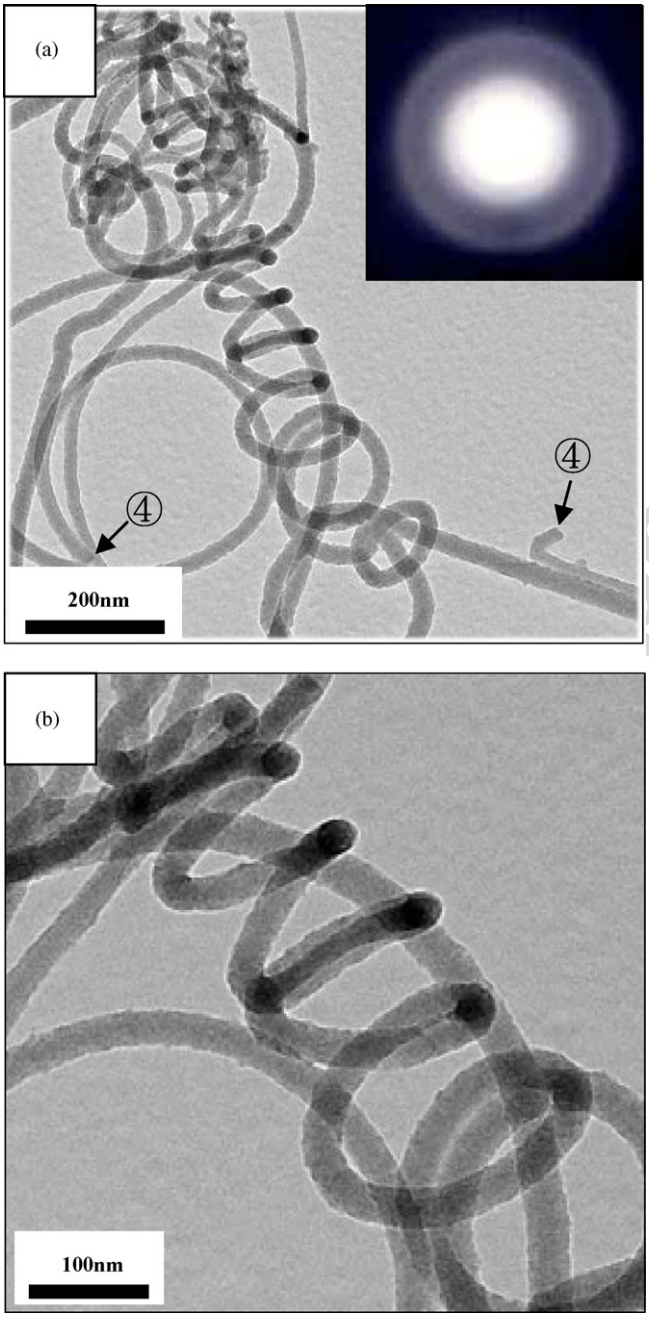

Fig. 2. (a) Low-magnification TEM image of the as-synthesized SiO_x nanostructures (inset: corresponding SEAD pattern). Arrow 4 indicates the tip part of the nanostructure. (b) TEM image of a nanospring.

Fig. 3a shows a TEM image of a nanoring, which is a helical nanostructure formed by multiple-loop rolling of a nanowire. The similar ring-like helical nanostructures were previously produced based on ZnO [9] and Si_3N_4 [14]. In addition, nanoparticle (indicated by arrow 5 in Fig. 3a) was observed at the end of the nanowire, appearing dark and having high contrast compared with the nanowire stem. A thin amorphous layer of 5–6 nm thickness exists on the surface of nanoparticle at the tip. EDX measurement made on the wire stem taken from an area indicated by arrow 6 reveals that the nanowire stem consists of Si and O (Fig. 3b). Cu and C signals are generated from microgrid mesh supporting the nanowires. EDX spectrum on the wire tip from the region indicated by arrow 5 in Fig. 3a shows the signals of Si, O, Cu, C, and Co elements (Fig. 3c). By

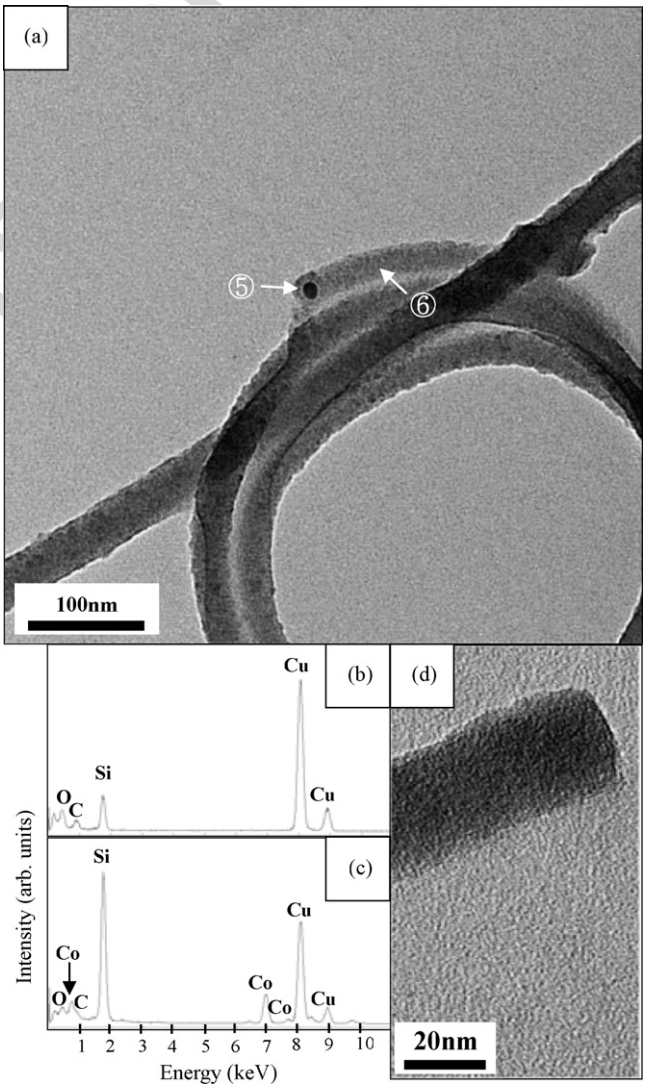

Fig. 3. (a) TEM image of a ring-like helical structure. EDX spectra of (b) the wire stem (arrow 6) and (c) the wire tip (arrow 5). (d) TEM image representing the tip part of a ring-like helical structure (corresponding to the region indicated by arrow 4 of Fig. 2a).

comparing Fig. 3c with b, although we do not know the exact chemical composition of the nanoparticle, we propose that the nanoparticle at least comprises a Co element.

Up to the present, various forms of SiO_x nanowires have been fabricated previously using the vapor–liquid–solid (VLS) method [12,23–29] or the vapor–solid (VS) process [30]. The solidified spherical droplet at the tip of the nanowires is commonly considered to be the evidence for the operation of the VLS mechanism. Fig. 3a shows the presence of tip nanoparticle in the present helical structures, possibly dismissing the growth mechanism mainly controlled by the VS process. However, in some instances, the Co catalyst nanoparticle was not present at the tips of the structures (Figs. 2a and 3d), suggesting that the Co-catalyst may stay at the bottom of the nanowires during the growth process. Hence, the growth mechanism of SiO_x nanowires cannot be ascribed to the commonly observed tip-growth VLS mechanism only, but also to the base-growth VLS mechanism. Similarly, previous work on the production of carbon nanotubes [31] and MgO nanowires [32] revealed that the growth can be ascribed to the base-growth mechanism, in which the metal catalyst remains situated at the bottom of the nanostructures.

Accordingly, the Co/Si droplets close to liquid phase will form at 1000 °C, evidenced by the observation that the Co-related nanoparticle has a spherical shape (Fig. 3a). Although the eutectic temperature of $CoSi_2$ (1259 °C [33]) is higher than the substrate temperature (1000 °C), the eutectic compound $CoSi_2$ may begin to form at a lower temperature, possibly due to the non-equilibrium processing condition and/or the melting effect of small-size grains of $CoSi_2$ islands, which was agglomerated from the thin (about 5 nm) Co layer. The liquid state particles should easily absorb oxygen and the presence of a relatively small amount of oxygen is not expected to change the Co–Si phase diagram significantly. As the droplets or particles become supersaturated, SiO_x nanowires are formed, possibly by the reaction between Si and O. The droplet will continuously absorb Si atoms as it is abundant in the system. Also, the O_2 in the carrier gas can supply a constant oxygen source during the process.

In our experimental process, due to the relatively low growth temperature (1000 °C), when the liquid Co–Si–O alloy drops become supersaturated with Si and O atoms, the re-crystallization of the atomic Si–O species is suppressed. Therefore, amorphous SiO_x nanowires tend to be generated instead of the crystalline nanowires, which is different from the growth of crystalline silicon nanowires [2,34]. There are two well-accepted mechanisms for the helical growth of ID nanostructures, viz. the contact angle anisotropy (CAA) and screw-dislocation mechanisms. From the observation that the helical nanostructures in the present study are amorphous, we can dismiss models based on lattice defects, such as screw-dislocation mechanism. Since the two underlying criterions that must be met in order to realize the CAA growth is that the structure of the helical nanowire is amorphous and that they grow by the VLS mode [14], we propose that the helical growth in the present study mainly follow the CAA mechanism. In all cases of helical growth, a mechanism must exist that introduces an asymmetry to the growth. In the case of helical nanostructures formed via the CAA growth, it is known that there exists contact angle anisotropy at the interface between the nanowire and the catalyst [15]. Further experimental study is needed to fine-tune the growth process and to clearly understand the growth mechanism of the helical nanostructures.

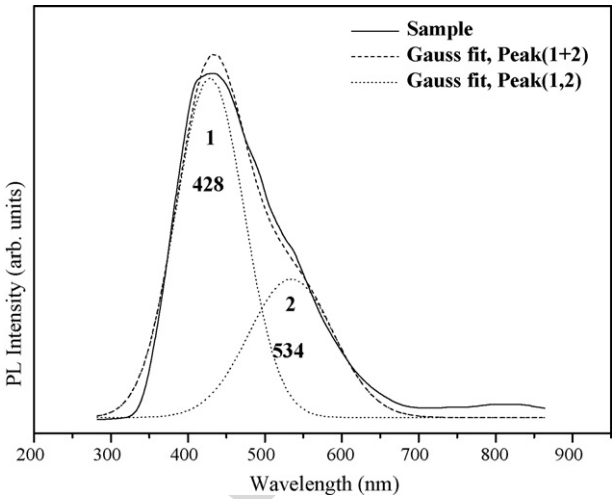

Fig. 4. PL of the SiO_x nanostructures, revealing the peaks at 428 and 534 nm, respectively.

The PL spectrum of the synthesized SiO_x nanostructures measured at room temperature is shown in Fig. 4, which is an apparent broad emission band mainly located in the visible region. Gaussian fitting analysis showed that the broad emission band was a superimposition of two major peaks at 428 and 534 nm, respectively. The similar blue emission with a peak position in the range of 414–470 nm have been previously observed in the PL spectrum of SiO_x nanowires [24,25,35,36], which was ascribed to neutral oxygen vacancy or oxygen deficiency-related diamagnetic defect centers [25]. Also, the similar green emission peaking at 540 nm has also been reported from the SiO_x nanowires [37], which has been ascribed to neutral oxygen vacancies [19]. We believe that both blue and green light emissions from the SiO_x nanostructures in the present study can be attributed to the above-mentioned defects arising from oxygen deficiency, presumably being generated during the high temperature synthetic process.

4. Conclusion

In summary, we have achieved the growth of SiO_x helical nanostructures through a Co-catalyzed process. SEM and TEM images indicate that the product comprises the spring- or ring-shaped helical nanostructures as well as the straight or slightly curved nanowires. The nanowires have diameters in the range of 20–100 nm. XRD and EDX analyses reveal that the nanowires are amorphous, consisting of silicon oxide. The growth of SiO_x nanostructures is most likely controlled by the extended VLS mechanism, in which Co-related catalytic particles are attached to the tips of some nanostructures. We suggest that the formation of amorphous SiO_x helical nanostructures can be explained in

terms of the CAA model. The room-temperature PL measurement with the Gaussian fitting shows apparent blue and green light emission bands centered at 428 and 534 nm, respectively.

Acknowledgement

This work was supported by INHA UNIVERSITY Research Grant.

References

[1] S. Iijima, Nature 354 (1991) 56.
[2] A. Morales, C.M. Lieber, Science 279 (1998) 208.
[3] W.I. Park, J.S. Kim, G.-C. Yi, H.-J. Lee, Adv. Mater. 17 (2005) 1393.
[4] L. Guo, J.X. Cheng, X.-Y. Li, Y.J. Yan, S.H. Yang, C.L. Yang, J.N. Wang, W.K. Ge, Mater. Sci. Eng. C 16 (2001) 123.
[5] X.Q. Chen, S.L. Zhang, D.A. Dikin, W.Q. Ding, R.S. Ruoff, L.J. Pan, Y. Nakayama, Nano Lett. 3 (2003) 1299.
[6] K. Kaneto, M. Tsuruta, S. Motojima, Synth. Met. 103 (1999) 2578.
[7] S. Motojima, M. Kawaguchi, K. Nozaki, H. Iwanaga, Appl. Phys. Lett. 56 (1990) 321.
[8] X.B. Zhang, X.F. Zhang, D. Bernaerts, G.T. Vantendeloo, S. Amelinckx, J. Vanlanduyt, V. Ivanov, J.B. Nagy, P. Lambin, A.A. Lucas, Europhys. Lett. 27 (1994) 141.
[9] X.Y. Kong, Z.L. Wang, Nano Lett. 3 (2003) 1625.
[10] P.X. Gao, Y. Ding, W. Mai, W.L. Hughes, C. Lao, Z.L. Wang, Science 309 (2005) 1700.
[11] L. Wang, D. Major, P. Paga, D. Zhang, M.G. Norton, D.N. Mcllroy, Nanotechnology 17 (2006) S298.
[12] H.-R. Zhang, C.-M. Wang, E.C. Buck, L.-S. Wang, Nano Lett. 3 (2003) 577.
[13] D. Zhang, A. Alkhateeb, H. Han, H. Mahmood, D.N. Mcllroy, M.G. Norton, Nano Lett. 3 (2003) 983.
[14] S. Motojima, S. Ueno, T. Hattori, K. Goto, Appl. Phys. Lett. 54 (1989) 1001.
[15] D.N. McIlroy, D. Zhang, Y. Kranov, M.G. Norton, Appl. Phys. Lett. 79 (2001) 1540–1542.
[16] S. Mann, G.A. Ozin, Nature 382 (1996) 313.
[17] A. Katz, M.E. Davis, Nature 403 (2000) 286.
[18] C.T. Kresge, M.W. Leonowicz, W.J. Roth, J.C. Vartuli, J.S. Beck, Nature 359 (1999) 710.
[19] H. Nishikawa, T. Shiroyama, R. Nakamura, Y. Ohiki, K. Nagasawa, Y. Hama, Phys. Rev. B 45 (1992) 586.
[20] L.S. Liao, X.M. Bao, X.Q. Zhang, N.S. Li, N.B. Min, Appl. Phys. Lett. 68 (1996) 850.
[21] D.S. Bethune, C.H. Kiang, M.S. De Vries, G. Gorman, R. Savoy, J. Vazquez, R. Beyers, Nature 363 (1993) 605.
[22] H.W. Kim, N.H. Kim, J.H. Myung, S.H. Shim, Phys. Stat. Sol. (a) 202 (2005) 1758.
[23] J.S. Wu, S. Dhara, C.T. Wu, K.H. Chen, Y.F. Chen, L.C. Chen, Adv. Mater. 14 (2002) 1847.
[24] Y.W. Wang, C.H. Liang, G.W. Meng, X.S. Peng, L.D. Zhang, J. Mater. Chem. 12 (2002) 651.
[25] D.P. Yu, Q.L. Hang, Y. Ding, H.Z. Zhang, Z.G. Bai, J.J. Wang, Y.H. Zou, W. Qian, G.C. Xiong, S.Q. Feng, Appl. Phys. Lett. 73 (1998) 3076.
[26] Z. Pan, S. Dai, D.B. Beach, D.H. Lowndes, Nano Lett. 3 (2003) 1279.
[27] J.C. Wang, C.Z. Zhan, F.G. Li, Solid State Commun. 125 (2003) 629.
[28] R. Ma, Y. Bando, Chem. Phys. Lett. 377 (2003) 177.
[29] S.H. Sun, G.W. Meng, M.G. Zhang, Y.T. Tian, T. Xie, L.D. Zhang, Solid State Commun. 128 (2003) 287.
[30] Y.F. Hao, G.W. Meng, C.H. Ye, L.D. Zhang, Appl. Phys. Lett. 87 (2005) 033106.
[31] S. Fan, M.G. Chapline, N.R. Franklin, T.W. Tombler, A.M. Cassell, H. Dai, Science 283 (1999) 512.
[32] H.W. Kim, S.H. Shim, Chem. Phys. Lett. 422 (2006) 165.
[33] T.B. Massalski, 1st ed., Binary Alloy Phase Diagrams, vol. 1, American Society for Metals, Metals Park, Ohio, 1986, p. 801.
[34] D.P. Yu, C.S. Lee, I. Bello, G.W. Zhou, Z.G. Bai, Z. Zhang, S.Q. Feng, Solid State Commun. 105 (1998) 403.
[35] Z.Q. Liu, S.S. Xie, L.F. Sun, D.S. Tang, W.Y. Zhou, C.Y. Wang, W. Liu, Y.B. Li, X.P. Zou, G. Wang, J. Mater. Res. 16 (2001) 683.
[36] G.Z. Ran, L.P. You, L. Dai, Y.L. Liu, Y. Lv, X.S. Chen, G.G. Qin, Chem. Phys. Lett. 384 (2004) 94.
[37] J.Q. Hu, Y. Jiang, X.M. Meng, C.S. Lee, S.T. Lee, Chem. Phys. Lett. 367 (2003) 339.